Techno-economic analysis of a bioethanol to hydrogen centralized plant

Journal:	*Energy & Fuels*
Manuscript ID	ef-2017-02434u.R1
Manuscript Type:	Article
Date Submitted by the Author:	n/a

Complete List of Authors:	Compagnoni, Matteo; Università degli Studi di Milano, Chemistry Mostafavi, Ehsan; Dep. of Chemical and Petroleum Engineering, Schulich School of Engineering, University of Calgary Tripodi, Antonio; Dept. Chemistry, Università degli Studi di Milano Mahinpey, Nader; University of Calgary Rossetti, Ilenia; Università degli Studi di Milano, Dip. Chimica

Techno-economic analysis of a bioethanol to hydrogen centralized plant

Matteo Compagnoni[a], Ehsan Mostafavi[b], Antonio Tripodi[a], Nader Mahinpey[b], Ilenia Rossetti[a,*]

(a) Chemical Plants and Industrial Chemistry Group, Dept. of Chemistry, Università degli Studi di Milano, CNR-ISTM and INSTM-Milano Università unit, Via C. Golgi 19, Milano, Italy

(b) Dep. of Chemical and Petroleum Engineering, Schulich School of Engineering, University of Calgary, Calgary T2N 1N4, Canada

ABSTRACT

The possibility to obtain chemicals and/or fuels from renewable sources is an attractive option in order to develop an integrated biorefinery concept. Bioethanol can be a suitable starting material for the production of H_2 as fuel or syngas. Hydrogen is considered as future energy vector that can meet the ever growing world energy demand in a clean and sustainable way. Moreover, it can be used as a green chemical for several other processes.

In this work, the centralized production of pure hydrogen from bioethanol was investigated using the process simulation software AspenONE Engineering Suite®. After designing the process and the implementation of kinetic expressions based on experimental data collected in our lab and derived from the literature, an economic evaluation and sensitivity analysis were carried out, assessing conventional economic indicators such as the net present value (NPV), internal rate of return (IRR) and pay-out period of the plant. In particular, three scenarios were studied by

* Corresponding author: fax +39-02-50314300; email ilenia.rossetti@unimi.it

changing the fuel of the furnace that heats up the ethanol steam reformer, *i.e.* using methane, ethanol or part of the produced hydrogen. Heat integration was also optimised for the best scenario.

Sensitivity analysis was applied to investigate the economic performance of bioethanol steam reforming under different circumstances, changing feedstock cost, hydrogen selling price, taxes and capital expenditure (CAPEX). The results highlight the advantages and drawbacks of the process on a large scale (mass flow rate of bioethanol 40,000 ton $year^{-1}$) for pure hydrogen production from bioethanol. The higher return is achieved when using methane as auxiliary fuel. The process was strongly OPEX sensitive and very tightly correlated to the bioethanol cost and hydrogen selling price.

Keywords*: Hydrogen Production; Bio-ethanol Steam Reforming; Economic evaluation; Biomass-derived Ethanol; Process Simulation; Heat Integration.*

1 - Introduction

The integrated biorefinery concept was introduced to match the future energy and environmental goals of our society. Renewable feedstocks are increasingly exploited for fuels and/or chemicals production [1]. Examples of biofuels are biodiesel [2] and bioethanol [3], whereas key biomass-derived chemicals are furans and polymers [4]. Moreover, the production of typical refinery products, *e.g.* bioethylene from the catalytic dehydration of bioethanol, can be implemented in an integrated biorefinery [5]. In addition, the interest on waste-based bio-refineries or waste-to-energy (WTE) is continuously on the raise as a solution to landfill waste problems, such as the case study reported by Nizami et al. for Saudi Arabia [6]. Sustainable hydrogen production is considered as one of the

most promising solutions to reduce the emissions in the automotive and industrial sectors, in some cases even being more energy efficient than traditional technologies [7,8]. Many scientific articles were published on the bio-ethanol steam reforming (BESR) process for hydrogen and syngas production, studying the catalyst [9,10], kinetic modeling [11–13] and technical feasibility for a large scale implementation [14]. However, only few studies on the cost-benefit analysis can be found in the open literature, which represents a limit to attract investments for deployment.

The operating pressure of BESR represents a first critical factor. The steam reforming reaction leads to an increase in the total number of moles; therefore, the higher is the pressure the lower is the advancement of the reaction at equilibrium (Le Chatelier principle). However, industrial natural gas steam reforming units conventionally operate at relatively high pressure (15-30 bar), because they supply hydrogen or syngas to processes operated at high pressure, *e.g.* ammonia, methanol, hydroformylation, Fischer-Tropsch synthesis, and it is more convenient to operate the steam reformer at a higher pressure than compressing the resulting syngas. Higher reformer pressure decreases the capital costs due to smaller reformer size and to lower compression costs to meet the specifications of the downstream processes [15–17]. Also when the process aims at centralized hydrogen production as fuel, the end user will need tank refill at high pressure, so that operating BESR at high pressure is advantageous. Thus, in this work a high-pressure reactor was designed, at difference with most literature on the topic.

Another critical point is the choice of the fuel for the furnace that supplies the energy needed by the reformer. In traditional methane steam reformers (MSR) the fuel is natural gas itself. Different options can be available for BESR, since bioethanol or part of the produced hydrogen/reformate can be used as fuels as well [18].

Several research groups investigated hydrogen combustion. Gallucci et al. studied the application of a dual fluidized-bed membrane reactor for hydrogen production via autothermal reforming of methane [19]. Part of the ultrapure hydrogen produced was sent to a burner to supply the energy required. Unfortunately, no economic assessment was proposed by the authors in order to establish the profitability of such choice. On the other hand, also the use of ethanol as fuel is feasible from the technical point of view [20]. The latter two approaches allow to avoid the carbon tax, because burning carbon-neutral bioethanol or green-hydrogen is considered neutral from the point of view of CO_2 emissions.

Nevertheless, the economic assessment of renewable hydrogen production units is insufficiently addressed in the literature. Indeed, even if some papers propose scale up and technical assessment of H_2 production units from renewables [17,21–23], solely one paper was focused on a techno-economic analysis of the simulated process [24] and none of them is related to the use of 2nd generation bioethanol.

For instance, Oakley et al. technically discussed the feasibility of BESR, but no economic analysis or process optimization were reported [14]. By contrast, Song et al. carried out an economic analysis about hydrogen production from bioethanol based on two plants of different sizes in the United States [24]. However, no pressure was specified for the process although this information is critical, as mentioned above.

A techno-economic analysis for the centralized hydrogen production from bioethanol can be an interesting case study to be compared with other emerging technologies, such as biomass gasification [8,25].

Therefore, the aim of this work is the techno-economic evaluation of a large scale bioethanol-steam-reforming plant for the production of pure hydrogen. The latter is intended for whichever use, as fuel or chemical. This step is a milestone to assess the feasibility of hydrogen production from bio-ethanol on a large scale, targeting the petroleum industry customers and large producers of bioethanol in the world.

2. Process Design and Modelling

2.1 – Process layout

The feasibility of power cogeneration through fuel cells using bioethanol at different concentration was already studied by us through an experimental apparatus for the combined heat and power cogeneration (5 $kW_{electrical}$ + 5 $kW_{thermal}$). The system was constituted by several reactors in series for hydrogen production (BESR), purification through High-Temperature Water Gas Shift (HT-WGS) + Low-Temperature Water Gas Shift (LT-WGS) + Methanation (Met) and by a fuel cell with the given power capacity [26].

In previous investigations [21,18,27] the process efficiency and the use of diluted bioethanol feeds were evaluated, considering different process configurations. However, the size of the fuel processor was suitable for a small-scale hydrogen production (6.5 Nm^3/h), needing proper upscaling in the present case. The same process layout was used, except that the fuel cells are not included here because not available commercially for a large power output. The big scale power generation using a gas-turbine or other types of fuel cells [23] was not considered, not to restrict the economic considerations. Indeed, the use of sustainable hydrogen for other chemical processes can be an intriguing alternative, as recently remarked by Schüth [4]: he underlined the use of

"renewable" hydrogen not only as energy vector, but also as a feedstock for the chemical industry, for oil refineries (hydro-treating processes), or in bio-refineries.

The fuel processor here proposed is constituted of a BESR steam reformer, a HT-WGS, a LT-WGS and a Met. Although in the literature CO-purification reactors are commonly simulated as Gibbs or equilibrium reactors, in this work we simulated them as fixed-bed reactors, by selecting and implementing kinetic expressions based on commercial catalysts, whereas for the BESR reactor a home developed kinetic model was used, relying on a proprietary catalyst. This allows the correct sizing of each reactor and, consequently, appropriate costing of each item.

The scheme of the process is sketched in Fig. 1. The feed for the steam reforming line is considered as a parallel alternative to the production of ethanol 99.5 Vol% (fuel grade, gray path in the Figure).

The BESR steam reformer was designed as a multitubular shell and tube reactor constituted by 100 tubes, 1 m long. In the tube side, an internal coating of active phase is loaded and the average temperature of the catalyst bed was 650°C. The shell side hosts the furnace flue gases. The high- and low-temperature water gas shift reactors are modelled as fized bed reactors, working at 350 and 280°C, respectively. The former converts ca. 90% of the CO outflowing the reformer, whereas the remaining portion is effectively removed by decreasing the temperature, so to favour the reaction thermodynamically. In order to deal with slower kinetics, a more active catalyst is selected for the low temperature stage (*vide infra*). The methanator accomplishes final CO removal below 20 ppm, operating at 210°C. This stage can be removed as redundant, if relying on CO separation in the following PSA unit is possible, *i.e*. whenever residual CO or improper purification is not too critical.

2.2 Modeling of the Reactors

The problem was assessed using the AspenONE Engineering Suite® (v. 8.6), in particular the flowsheet has been designed and optimized using the Aspen Plus® process simulator, whereas the economic analysis was carried out using the Aspen Process Economic Analysis module.

The chemical process design was performed using the traditional hierarchical method (onion model) [28]. The reactor was the starting point of the design, followed sequentially by the separation and purification units.

The kinetic expression for the steam reforming reaction was already presented in a previous work [18]. The kinetic model here used was originally developed for a $Rh/MgAl_2O_4/Al_2O_3$ catalyst [29] and includes 14 elementary steps, 4 of which were proposed as rate determining ones: ethanol decomposition (ED), ethanol steam reforming (SRE), methane steam reforming (SRM) and water gas shift (WGS). The kinetic equations were based on a Langmuir Hinshelwood approach, where all the species concurring for adsorption over the active sites appear in the denominator of the rate expressions and are included in the overall balance on the active sites. This model has been adapted by us [27] to a full set of experimental data collected for a commercial Ni/Al_2O_3 sample [30] and later to our home-developed catalyst [12,31]. In the present work we preferred to deal with the kinetic model detailed in [27] because it is specifically used to describe the commercial Ni-based catalyst, which is more pertinent for the present application.

For the HT-WGS step the kinetics proposed by Hla et al. [32] was selected. The power-law reaction rate expressions were proposed for a commercial $Fe_2O_3/Cr_2O_3/CuO$ catalyst.

The catalytic fixed-bed reactor for the LT-WGS step was simulated selecting the work of Choi et al. [33]. A Commercial $Cu/ZnO/Al_2O_3$ catalyst was employed and, also in this case, the authors applied a power-law reaction rate expression.

For the CO methanator, the article of Zhang et al. [34] reported the use of a commercial Ni/Al_2O_3 catalyst, following a Langmuir-Hinshelwood-Hougen-Watson kinetic expression (LHHW). The reactions considered, model adopted and references are summarised in Table 1. The parameters to calculate the equilibrium constants were obtained following Bartholomew and Farrauto [35].

The experimental steam reformer tested in-house [18,27] was configured as a shell and tubes heat-exchanger, where the steam reforming catalyst was located in tube side and a commercial combustion catalyst in the shell side. The catalysts can be present as coating to optimize the thermal coupling [26] or alternatively as particles in fixed-bed [10].

However, this configuration was changed in this case due to the unproven commercial feasibility of this thermally optimized approach for larger design and the reactor was sized based on the industrial terrace wall steam reforming reactor [36]. The sizing parameters are reported in Table 2. For the main steam reforming unit the particle size and pressure drop were simulated in detail considering the shape factor (0.58), Sauter particle diameter (12.5 mm) and an overdesign factor of 20%. The same number of tubes and length/internal diameter ratio of the experimental configuration were adopted [37]. Particle shape was simulated as a single-channel cylinder (ring shape). The pressure profile along the catalyst bed has been calculated according to the Ergun equation. The water gas shift reactors and methanator were simulated considering their typical commercial features [38,39], in adiabatic configuration which is the more acceptable for industrial applications compared to the isothermal one [35]. A scale-up ratio of 1800 based on the ethanol stream was used assuming a capacity of 40,000 ton/y of bioethanol. This productivity has been

chosen based on a commercial examples of second generation bioethanol production plant currently commercialized by the Biochemtex group [40]. The vaporized feed was simulated by feeding high pressure liquid ethanol and water mixture into a vaporizer.

Usually, hydrogen production by steam reforming of ethanol is experimentally investigated at pressures below 10 bar [10,41,42]. However, the implementation for large scale production must be explored in the pressure range at which steam reforming of natural gas for syngas generation is economically viable, which is higher than 10 bar [14]. Thus, a pressure of 20 bar was here chosen in order to match the balance between compression cost, equipment volume and thermodynamic conversion. In addition, further increasing pressure can lead to inconsistent results based on low pressure kinetics. Thermal gradient through the catalytic bed was simulated as for the experimental unit.

The water/ethanol ratio was thoroughly optimized recently [43]: the higher the ratio, the higher is the hydrogen yield due to promotion of the WGS reaction, with consequent mitigation of the impact of the hydrogen purification sequence. Excess water also prevents effectively catalyst deactivation by coking [44]. As a counterbalance, increasing heat input is required to vaporize additional water. In this work, an optimal steam-to-ethanol molar ratio equal to 5 was selected (40 vol% Ethanol, 60 vol% Water). This composition is easily achievable either by partially purifying the bioethanol raw beer by flash or by using a feed split approach as extensively described elsewhere [45,46]. in order to use a feasible bioethanol stream. Finally, we compared the present results with those reported by Oakley et al., who simulated the process on an industrial scale, but without implementing kinetic expressions [14].

2.3 - Modelling the Process

The flowsheet is reported in Fig. 2. Heaters and coolers were simulated by setting the utilities and surface area reported in Table 3.

The furnace coupled to the steam reformer, was simulated in Aspen Plus® using a Gibbs reactor. The mass flowrates of air and fuel where adjusted so to generate the heat duty needed by the reactor with an air flowrate leading to 2% excess oxygen with respect to the stoichiometric [47]. A firebox reformer heater (rectangular shape) without catalyst was selected for the economic evaluation, with walls externally lined by refractory material.

The compressors for air and fuel were simulated in accordance with the Gas Processors Suppliers Association (GPSA) standards. The reciprocating configuration coupled with gas engine was chosen. The pumps were simulated using centrifugal configuration.

The Pressure Swing Adsorption (PSA) unit was simulated in accordance with a traditional H_2 recovery unit typically used for refinery off-gas streams [48]. This reference work was chosen based on the similar pressure range (20 bar) and temperature (308 K), although a higher steam molar flow was used in our case. The amount of zeolite was scaled up accordingly. The four units of PSA were considered operating in parallel as detailed by Mivechian et al. [48]. The storage tanks and other offsite equipment were not included in the assessment. The plant flowsheet was established based on experiments in a 13.9 kg/d pilot plant, including purification steps of WGS and methanation, but without a PSA unit.

2.4 - Modeling the Heat-Exchangers Network

The heat integration was implemented using the Aspen Energy Analyzer® tool using the pinch analysis methodology. This technique analyses all the thermal flows within the process boundaries, identifying the most economical ways to maximize the heat recovery and minimise the demand for external utilities. Heat exchangers were sized calculating the heat exchange surface area using conventional industrial considerations in order to properly choose the location of the fluids (shell or tube side) and the other critical parameters such as fouling, phase change, erosion and corrosion. The flowsheet after the heat integration is detailed in Fig. 3, whereas the specifications of the heat exchangers used for process and relative diagram are shown in the Supporting Information file (Table S1 and Fig. S1).

3. Economic Performance Analysis

The simulated process flowsheet was used to estimate the Total Capital Investment (TCI) and the OPerating EXpenditures (OPEX) of the hydrogen production and purification sections. Different scenarios and price sensitivity analyses were defined to highlight the dependence of CAPEX and OPEX on different economic parameters.

3.1. Economic Assumptions

The economic assumptions are listed in Table 4. A rate of return of 10 was chosen as profitability factor. A 30 year plant life was assumed, based on similar steam reforming technologies [24,49]. The working capital was assumed as 15% of the TCI as conventionally used for traditional chemical plants [28]. The salvage value was evaluated as a fraction of the initial capital cost. The straight-line method was adopted as depreciation method (the difference

between the salvage value and the initial capital was divided by the economic life of the project, so that the project depreciates evenly through all its economic life).

For both the product and the raw materials we considered the same escalation value (= 5), as reasonable because these compounds pertain to the commodity market. The stream factor was set to 96% (8406 operating hours per year).

The choice of raw materials costs, utility cost and product selling price is always a critical point for the economic evaluation of a project, because it heavily influences the outputs of the analysis. This point is a minor issue when the scope is the internal comparison of different scenarios under the same assumptions. On the contrary, it is important for the comparison with literature data or with existing plants. The price of bioethanol was estimated considering a commercial selling price of pure bioethanol [40] diminished by 50% due to savings in the purification by flash or feed split with respect to the azeotropic distillation [18,27,46,37]. Indeed, the purification of bioethanol can affect up to 50-80 % its production price, at least for the first generation biofuel [46,50].

The ASME Boiler & Pressure Vessel Code (BPVC) were chosen as the standard for the design of pressure vessels. Feedstock, utility and product costs are summarized in Table 5.

Catalysts were considered in CAPEX and not in OPEX because the reactors considered to have fixed-bed configuration, therefore there is no need of continuous make up of fresh catalyst to the reactor. Catalyst deactivation issues were also computed and mainly ascribed to sintering and coking, with lower impact of the latter because of the high temperature of reaction [10]. Planned shutdowns of the plant were predicted for the regeneration.

3.2. Investment Calculation Criteria and Methodology

The following equations have been used for calculations:

$$NPV = \sum_{k=1}^{n} \frac{CF}{(1+i)^n}$$

NPV = Net Present Value, where *n* is the project lifetime (or economic life of the project), CF is the annual cash flow and *i* is the interest rate (also called desired rate of return or return on investment, ROI). NPV measures the difference between the present value of cash inflows and the present value of cash outflows. It is used in capital budgeting to analyze the profitability of a projected investment or project. On the other hand, ROI is a performance measure to evaluate the efficiency of an investment or to compare the efficiency of a number of different investments. ROI measures the amount of return on an investment relative to the investment's cost.

The IRR (Internal Rate of Return) was then evaluated as the interest rate at which the present value in the last year of the project is zero, obtained by solving the following implicit equation.

$$NPV = \sum_{k=1}^{n} \frac{CF}{(1+IRR)^n} = 0$$

The IRR is a metric used in capital budgeting measuring the profitability of potential investments. It is a discount rate that makes the NPV of all cash flows from a particular project equal to zero. The total capital cost (C_T) was evaluated using the Aspen Process Energy Analyzer (APEA) library at the system cost base date, adjusted to the present date using the capital escalation values reported in Table 4, according to the following equation.

$$C_{AT} = C_T * \left(1 + t_D * \left(\frac{e}{100}\right)\right)$$

C_{AT} = Adjusted Total Capital cost; t_D = Time difference between system cost base date and start date for engineering; e = Project capital escalation. The project capital escalation was chosen considering the chemical engineering plant cost indices during the last years.

The economic analysis was carried out at first considering a fixed H_2 selling price and a fixed ROI. The operating costs were evaluated including the following items: raw materials, G&A expenses (general and administrative costs), operating labor costs, plant overheads, charges during production for services (facilities, payroll overhead, etc.), utilities, maintenance.

The starting date for the calculation of operating costs was the day after the end of the Engineering-Procurement-Construction (EPC) phase. The starting date for the calculation of product sales was the day after the end of the EPC + start-up phases. The final cash flow at the end of plant life was calculated based on the salvage value and the working capital in addition to the total earnings.

Aspen Process Economic Analyzer was used to identify a window of economic viability of the process considered. This tool enables to focus the engineering process on business priorities, integrating business considerations and sophisticated engineering analysis. All the results were checked, re-evaluated and compared with the literature [28] and industrial case histories.

4. Results and Discussion

4.1 Economic analysis of different scenarios

A first economic assessment was carried out using methane as fuel for the furnace and excluding any heat-integration (base case). Fig. 4 shows the CAPEX evaluation for this scenario,

considering the capital fraction relative to the equipment. The highest issues are related to the heater for the vaporization of the feed, followed by the compressors and the steam reforming units (inluding the shell and tubes reactor plus the furnace). OPEX are shown in the same Fig. 4 and evidence that bio-ethanol, even if diluted and less expensive than the azeotrope, still represents the major cost, followed by methane (fuel for the furnace). The flowrate of pure hydrogen at the outlet of PSA is 889 kg h^{-1}. This value was obtained by feeding 4,567 kg h^{-1} (40,000 ton $year^{-1}$) of ethanol.

Three different scenarios (A, B, C) where then compared: the base case above discussed relies on methane as fuel for the furnace (case A), while using as fuel pure ethanol (case B) or a portion of the produced hydrogen-rich stream (case C) were considered as alternatives. The flowsheet for cases B and C are reported in the Supplementary Information for completeness (Fig. S2 and S3).

The comparison of total CAPEX (considering working capital, direct costs and equipment costs) and total OPEX (considering raw materials, operating labor costs, utilities, G&A expenses) for the three scenarios is reported in Fig. 5.

Capital costs were slightly lower for scenario C because no compressor was needed for the already pressurized hydrogen when used as fuel. By contrast, OPEX assume markedly different values for every scenario. Scenario B has the highest OPEX, because the furnace is fed with pure ethanol (azeotrope), which is assumed as much more expensive than the diluted bioethanol used as feed. This demonstrated as a valid and less expensive alternative to anhydrous ethanol for steam reforming, even for the production of bioethylene [5,43,46,51]. However, the use of the diluted bioethanol to feed the burner is precluded by its insufficient heating value. On the other hand, the lowest value for OPEX is achieved for case C, because no additional fuel is used. However, it

considerably shortens product sales, because part of the product is internally used for heating, and, thus, total plant revenues.

The Internal Rate of Return (IRR) measures efficiently how the capital is being used, although it gives no indication on the profits. In this comparison, the IRR is 24.9%, 14.9% and 0% for the scenarios A, B and C, respectively. The possibility to use part of the hydrogen produced as fuel for the thermal supply of the endothermal process was investigated in a thermodynamic study by Giunta et al. [22]. Although the study was not aimed to discuss the economic advantages of the choice, the study interestingly supported some of the conclusions achieved in our previous work, where the use of the produced reformate for internal heat generation was extensively investigated in a small scale heat and power cogeneration plant (5 $kW_{electrical}$ + 5 $kW_{thermal}$) [18]. However, the null value of IRR here obtained means that the investment is not profitable on a large industrial scale to get revenues. Nevertheless, scenario C may keep its interest on a small scale for independent residential cogeneration, where the exploitation of other fuels may be excluded for different reasons.

Additionally, scenario B was less remunerative than A, due to the higher price of ethanol than methane and higher energy needed to vaporize of the fuel. Moreover, in this case complications arise with furnace optimization when using ethanol instead of the very well assessed methane-based technology.

4.2 Thermal integration of the process

The energy integration of the best scenario (A) was performed, at first by categorizing the hot and cold streams and then making a pinch analysis to design the heat exchangers network. A

first, rather conventional solution for heat integration is to thermally couple the reactor feed and product stream. A preheating train of heat exchangers was then designed, taking advantage of the fact that the whole separation unit operations operates in decreasing cascade temperature with respect to the reactor. The pinch point was found and several scenarios of integration were compared. The heat exchanger network was then designed accordingly.

The optimal integration scenario in terms of both minimum exchanger cost and utility consumption was implemented in the final simulation. Nevertheless, this part of the utilities design can be further optimized case by case considering the context of the site, with possibly coexisting processes that can be also connected to a common utility system. After the heat integration, the new partition of CAPEX is reported in Fig. 6.

The comparison of CAPEX and OPEX before and after heat integration is reported in Fig.7. CAPEX increased upon heat integration, due to additional equipment and higher system complexity. By contrast, OPEX were of course lower in the heat integrated case, due to lower external utilities. The real advantages in terms of economic expenditure after the heat integration were deepened by evaluating again NPV, IRR and the Pay-out period (Table 6).

Both the NPV (absolute profit) and the IRR (efficiency of capital return) increased after heat integration. Of course these two parameters alone have limits, for example they do not consider the time value of money and are based on average operations during time, excluding important issues such as the variation of maintenance costs over the project life, changing sales volume and so on [28]. In spite of this, they work very well for a general comparison among different projects. Overall, the advantage of reducing OPEX was predominant over the disadvantage of higher capital costs.

The further conversion of CO to CO_2 after the HTS stage could be considered apparently worthless because the remaining small amount of CO is feasible for the separation with the PSA unit. However, this plant design choice was maintained because the integration of CO_2 capture technologies in the process require the larger concentration possible of CO_2 to enhance the efficiency [8,25].

Finally, it should be underlined that that no CO_2 selling option has been here included, that would add revenues, but also installation and operation costs. In case, a CO_2 capture unit can be easily implemented because the outlet stream from the PSA unit has the 92% in mass of CO_2 and just the 8% of methane, but it is out off-topic for this work.

4.3 Sensitivity analysis

A sensitivity analysis was performed to quantify the dependence on changes in market price of raw materials and products (Fig. 8).

The process revealed poorly sensitive to taxes and CAPEX variation, whereas changing the ethanol cost was very critical. Its cost strictly depends on the starting biomass and on the purification strategy (use of more or less diluted bioethanol). For this reason, bioethanol, as emerging source for energy production, may show higher price volatility than other chemicals. This point further stresses the need to propose cost-effective routes to diluted bioethanol.

In our hypothesis, we used the cost of commercial 2^{nd} generation ethanol, assuming a 50% reduction of the diluted ethanol price with respect to the pure one. This choice can be considered one of the worst scenarios possible because of two main reasons: i) 2^{nd} generation bioethanol (obtained by lignocellulosic biomass, agricultural residues or waste) is more expensive and more

difficult to obtain than 1st generation bioethanol (mainly produced from corn and sugar cane) [52]; ii) the purification of bioethanol may affect up to 50-80% the ethanol production price [50,53]. The upstream biochemical processes (*e.g.* enzymatic hydrolysis, microbial fermentation, biomass pretreatments) were not investigated in this work, making reference to existing papers on the topic [54,55]. We are basing this analysis on the existing selling costs of second generation bioethanol, but it can be easily adapted to 1st generation feedstock, with consistent savings.

However, even if no significant cost saving would derive from the use of diluted ethanol (Fig. 8B, case with ethanol cost +50%), the system remains profitable, with IRR after taxes still sufficiently higher than 15%.

This analysis concludes that the process is not very sensitive to CAPEX, but it is instead markedly OPEX sensitive. Indeed, besides ethanol cost, hydrogen selling price represents the most critical parameter affecting both NPV and IRR.

Finally, the process studied is totally carbon free if fuels at the furnace are ethanol or hydrogen, instead in the case of methane the CO_2 produced by the combustion must be taken into account. The influence of this point on the total OPEX was evaluated considering the worst scenario found in literature (carbon tax equal to 10 USD/tonCO_2) and revealed an influence of 1.55% on the total operative expenditure (19.4 kton/y of CO_2 produced by the furnace). A further sensitivity analysis considering the variability of this tax due to the different values related to the country policy and regulations was avoided due to the low impact of this item on the total cost.

At last, by selecting the optimized heat integrated process, using methane as fuel utility and selecting an internal rate of return of 10% (which results in a NPV of zero at the end of the project life), the calculated minimum hydrogen selling price would be 1.91 USD/kg, to be

compared with a present standard value from methane steam reforming of 1.80 USD/kg [56]. This calculation was made for a system capable of producing 7,793 ton/y of H_2 (9,886 Nm^3 h^{-1}) starting from 40,000 ton/y of bioethanol.

5. Conclusions

The exploitation of bioethanol steam reforming technology for the production of hydrogen on a large commercial scale was evaluated through process design and techno-economic analysis. This proposed process offers a novel carbon neutral technology that can be utilized in bio-refineries. A comprehensive simulation, heat integration and equipment sizing was performed aiming at economic assessment of this bioethanol-to-hydrogen route.

Three scenarios were investigated showing that hydrogen production is economically feasible from bioethanol. The most remunerative option was obtained using methane as a fuel for the reforming furnace (NPV equal to 50.8 x 10^6 USD after 30 years, pay-back period 7.3 years, IRR 24.9% after taxes). Also the use of azeotropic bioethanol could be considered economically feasible although less remunerative in terms of economic investment. Heat integration was also successfully applied further increasing the IRR (from 24.9% to 27.1%) and decreasing the pay-back period (from 7.3 to 6.6 years). The economic sensitivity analysis revealed the OPEX sensitive nature of the process, in particular considering the feedstock cost (ethanol) and hydrogen selling price.

This study wishes to fill the gap in the literature about the economic assessment of real bioethanol steam reforming implementation on already existing industrial fermentative plants. The study fixes the fundamentals to compare this option from an economic point of view other

technologies for bioethanol valorization in biorefineries and for hydrogen production from renewables. For example, the ethylene production by dehydration and subsequent polymerization, the use of green hydrogen for the reduction of lignin to produce aromatic compounds or the use of hydrogen for side hydrogenation processes.

References

(1) Mazzetto, F.; Simoes-Lucas, G.; Ortiz-Gutiérrez, R. A.; Manca, D.; Bezzo, F. *Chem. Eng. Res. Des.* **2015**, *93*, 457–463.

(2) Vlysidis, A.; Binns, M.; Webb, C.; Theodoropoulos, C. *Energy* **2011**, *36* (8), 4671–4683.

(3) Chaichanawong, J.; Yamamoto, T.; Ohmori, T.; Endo, A. *Chem. Eng. J.* **2010**, *165* (1), 218–224.

(4) Schüth, F. *Catal. Hydrog. Biomass Valorization* **2015**, No. 13, 1–21.

(5) Rossetti, I.; Compagnoni, M.; Finocchio, E.; Ramis, G.; Di Michele, A.; Millot, Y.; Dzwigaj, S. *Appl. Catal. B Environ.* **2017**, *210*, 407–420.

(6) Nizami, A. S.; Shahzad, K.; Rehan, M.; Ouda, O. K. M.; Khan, M. Z.; Ismail, I. M. I.; Almeelbi, T.; Basahi, J. M.; Demirbas, A. *Appl. Energy* **2017**, *186*, 189–196.

(7) Díaz Alvarado, F.; Gracia, F. *Chem. Eng. J.* **2010**, *165* (2), 649–657.

(8) Esmaili, E.; Mostafavi, E.; Mahinpey, N. *Appl. Energy* **2016**, *169*, 341–352.

(9) Mattos, L. V.; Jacobs, G.; Davis, B. H.; Noronha, F. B. *Chem. Rev.* **2012**, *112* (7), 4094–4123.

(10) Compagnoni, M.; Lasso, J.; Di Michele, A.; Rossetti, I. *Catal. Sci. Technol.* **2016**, in press.

(11) Compagnoni, M.; Tripodi, A.; Rossetti, I. *Appl. Catal. B Environ.* **2016**, *203*, 899–909.

(12) Tripodi, A.; Compagnoni, M.; Rossetti, I. *ChemCatChem* **2016**, 1–11.

(13) Akande, A.; Aboudheir, A.; Idem, R.; Dalai, A. *Int. J. Hydrogen Energy* **2006**, *31* (12), 1707–1715.

(14) Oakley, J. H.; Hoadley, a. F. a. *Int. J. Hydrogen Energy* **2010**, *35* (16), 8472–8485.

(15) Rossetti, I.; Pernicone, N.; Ferrero, F.; Forni, L. *Ind. Eng. Chem. Res.* **2006**, *45* (12), 4150–4155.

(16) Luyben, W. L. *Ind. Eng. Chem. Res.* **2010**, *49*, 6150–6163.

(17) Baltrusaitis, J.; Luyben, W. L. *ACS Sustain. Chem. Eng.* **2015**, *3* (9), 2100–2111.

(18) Rossetti, I.; Compagnoni, M.; Torli, M. *Chem. Eng. J.* **2015**, *281*, 1036–1044.

(19) Gallucci, F.; Van Sint Annaland, M.; Kuipers, J. A. M. *Top. Catal.* **2008**, *51* (1–4), 133–145.

(20) Mujeebu, M. A.; Abdullah, M. Z.; Bakar, M. Z. A.; Mohamad, A. A.; Abdullah, M. K. *Prog. Energy Combust. Sci.* **2009**, *35* (2), 216–230.

(21) Galera, S.; Gutiérrez Ortiz, F. J. *Fuel* **2015**, *144*, 307–316.

(22) Giunta, P.; Mosquera, C.; Amadeo, N.; Laborde, M. *J. Power Sources* **2007**, *164* (1), 336–343.

(23) Spallina, V.; Pandolfo, D.; Battistella, A.; Romano, M. C.; Van Sint Annaland, M.; Gallucci, F. *Energy Convers. Manag.* **2016**, *120*, 257–273.

(24) Song, H.; Ozkan, U. S. *Int. J. Hydrogen Energy* **2010**, *35* (1), 127–134.

(25) Mostafavi, E.; Sedghkerdar, M. H.; Mahinpey, N. *Ind. Eng. Chem. Res.* **2013**, *52* (13), 4725–4733.

(26) Rossetti, I.; Biffi, C.; Tantardini, G. F.; Raimondi, M.; Vitto, E.; Alberti, D. *Int. J. Hydrogen Energy* **2012**, *37* (10), 8499–8504.

(27) Rossetti, I.; Compagnoni, M.; Torli, M. *Chem. Eng. J.* **2015**, *281*, 1024–1035.

(28) Peters, M. S.; Timmerhaus, K. D. *Plant design and economics for chemical engineers*; 1991.

(29) Graschinsky; Laborde; Amadeo; Valant, L.; Blon; Epron; Duprez. *Eng Chem Res* **2010**, *49*.

(30) Mas, V.; Bergamini, M. L.; Baronetti, G.; Amadeo, N.; Laborde, M. *Top. Catal.* **2008**, *51* (1–4), 39–48.

(31) Compagnoni, M.; Tripodi, A.; Rossetti, I. *Appl. Catal. B Environ.* **2017**, *203*, 899–909.

(32) Hla, S. S.; Park, D.; Duffy, G. J.; Edwards, J. H.; Roberts, D. G.; Ilyushechkin, A.; Morpeth, L. D.; Nguyen, T. *Chem. Eng. J.* **2009**, *146* (1), 148–154.

(33) Choi, Y.; Stenger, H. G. *J. Power Sources* **2003**, *124* (2), 432–439.

(34) Zhang, J.; Fatah, N.; Capela, S.; Kara, Y.; Guerrini, O.; Khodakov, A. Y. *Fuel* **2013**, *111*, 845–854.

(35) Bartholomew, C. H.; Farrauto, R. *Fundamentals of Industrial Catalytic Processes*; John Wiley & Sons, 2011.

(36) Mohammadzadeh, S.; Zamaniyan. *Chem. Eng. Res. Des.* **2002**, *80* (4 A), 383–390.

(37) Tripodi, A.; Compagnoni, M.; Ramis, G.; Rossetti, I. *Int. J. Hydrogen Energy* **2017**, *42* (37), 23776.

(38) Er-rbib, H.; Bouallou, C. *Chem. Eng. Trans.* **2013**, *35*, 541–546.

(39) Criscuoli, A.; Basile, A.; Drioli, E.; Loiacono, O. *J. mem* **2001**, *181*, 21–27.

(40) www.Biochemtex.com.

(41) Cavallaro, S. *Energy & Fuels* **2000**, *14*, 1195–1199.

(42) Hou, T.; Zhang, S.; Chen, Y.; Wang, D.; Cai, W. *Renew. Sustain. Energy Rev.* **2015**, *44*, 132–148.

(43) Tripodi, A.; Compagnoni, M.; Ramis, G.; Rossetti, I. *Int. J. Hydrogen Energy* **2017**, in press.

(44) Ramis, G.; Rossetti, I.; Finocchio, E.; Compagnoni, M.; Signoretto, M.; Michele, A. Di. In *Progress in clean energy*; 2015; Vol. 1, pp 695–711.

(45) Ramis, G.; Rossetti, I.; Tripodi, A.; Compagnoni, M. *Chem. Eng. Trans.* **2017**, *57*, 1663–1668.

(46) Rossetti, I.; Lasso, J.; Compagnoni, M.; Guido, G. De. *Chem. Eng. Trans.* **2015**, *43* (2013), 229–234.

(47) Luyben, W. L. *J. Process Control* **2016**, *39*, 77–87.

(48) Mivechian, A.; Pakizeh, M. *Chem. Eng. Technol.* **2013**, *36* (3), 519–527.

(49) Cormos, A.-M.; Cormos, C.-C. *Int. J. Hydrogen Energy* **2016**, 1–13.

(50) Lee, F.; Pahl, R. H. *Ind. Eng. Chem. Process Des. Dev.* **1985**, *24* (1), 168–172.

(51) Rossetti, I.; Compagnoni, M.; De Guido, G.; Pellegrini, L.; Ramis, G.; Dzwigaj, S. *Canad. J. Chem. Eng.* **2017**, *95*, 1752.

(52) Baladincz, P.; Hancsòk, J. *Chem. Eng. J.* **2015**, *282*, 152–160.

(53) Kazi, F. K.; Fortman, J. A.; Anex, R. P.; Hsu, D. D.; Aden, A.; Dutta, A.; Kothandaraman, G. *Fuel* **2010**, *89* (SUPPL. 1), S20–S28.

(54) Nasidi, M.; Akunna, J.; Deeni, Y.; Blackwood, D.; Walker, G. *Energy Environ. Sci.* **2010**, *3* (10), 1447.

(55) Unrean, P.; Khajeeram, S. *Renew. Energy* **2016**, *99*, 1062–1072.

(56) Bornapour, M.; Hooshmand, R. A.; Khodabakhshian, A.; Parastegari, M. *Appl. Energy* **2017**, *202*, 308–322.

TABLES

Table 1. Kinetic expressions implemented in the fixed-bed reactors.

Process	Reaction	Kinetic model type	Ref.
Steam Reforming	$CH_3CH_2OH \rightarrow CH_4 + CO + H_2$ $CH_3CH_2OH + H_2O \rightarrow CO_2 + CH_4 + 2H_2$ $CH_4 + H_2O \leftrightarrows CO + 3H_2$ $CO + H_2O \leftrightarrows CO_2 + H_2$	LHHW	[18,27]
HT-WGS	$CO + H_2O \leftrightarrows CO_2 + H_2$	Power-law	[32]
LT-WGS	$CO + H_2O \leftrightarrows CO_2 + H_2$	Power-law	[33]
Methanation	$CO + 3H_2 \leftrightarrows CH_4 + H_2O$	LHHW	[34]

Table 2. Design parameters of the reactors.

Parameter	**SR**	**HT-WGS**	**LT-WGS**	**MET**
Catalyst	Ni/Al_2O_3	$Fe_2O_3/Cr_2O_3/CuO$	$Cu/ZnO/Al_2O_3$	Ni/Al_2O_3
GHSV (h^{-1})	7,700	10,600	6,800	3,900
Mass of catalyst (kg)	4,078	3,197	4,984	5,406
Particle density (kg/m^3)	2,356	1,630	1,630	1,014
L/D	43	2.8	1.4	2.0
Number of tubes	109	1	1	1

Table 3. Specifications of heat exchangers used for process before heat-integration (base case).

Item	Heater-1	Cooler-1	Cooler-2	Cooler-3	Cooler-4	Cooler-5
Utility	Fired Heater	High Pressure Steam Generation	Cooling Water	Cooling Water	Cooling Water	Cooling Water
Heat Duty (MW)	12.89	-4.54	-1.35	-0.82	-4.88	-5.96
Area (m^2)	1533.0	46.6	72.6	9.4	66.3	21.0

Table 4. Investment Parameters.

Parameter	Unit of measure	Value
Corporate tax rate	%	30
Interest rate / Desired rate of return	%	10
Economic life of the project	year	30
Salvage Value (fraction of initial capital cost)	%	20
Capital escalation (e)	%	2
Products escalation	%	5
Raw Materials escalation	%	5
Operating and maintenance labor escalation	%	3
Utilities escalation	%	3
Working Capital (WC)	%	15
Start-up period	week	20
G&A expenses	%	8
Operating hours per year	hour	8406

Table 5. Feedstock, utility and product costs.

Parameter	Unit	Price
Bioethanol (40 vol.%)	USD/kg	0.211
Methane	USD/m^3	0.177
Water	USD/kg	0.118
Electricity	USD/kWh	0.0775
Hydrogen	USD/kg	2.69

Table 6. Economic evaluation of the scenario A before and after heat integration (HI).

	NPV after 30 years	Pay-out period	IRR after taxes
	10^6 USD	Year	%
Before HI	50.8	7.3	24.9
After HI	62.2	6.6	27.1

FIGURES

Fig. 1. Scheme of two parallel routes to exploit bioethanol produced by fermentation. 1st route: centralized hydrogen production; 2nd route: production of 99.5 Vol.% ethanol for the liquid fuel market. WGS = Water Gas Shift; Met = Methanation; PSA = Pressure Swing Adsorption.

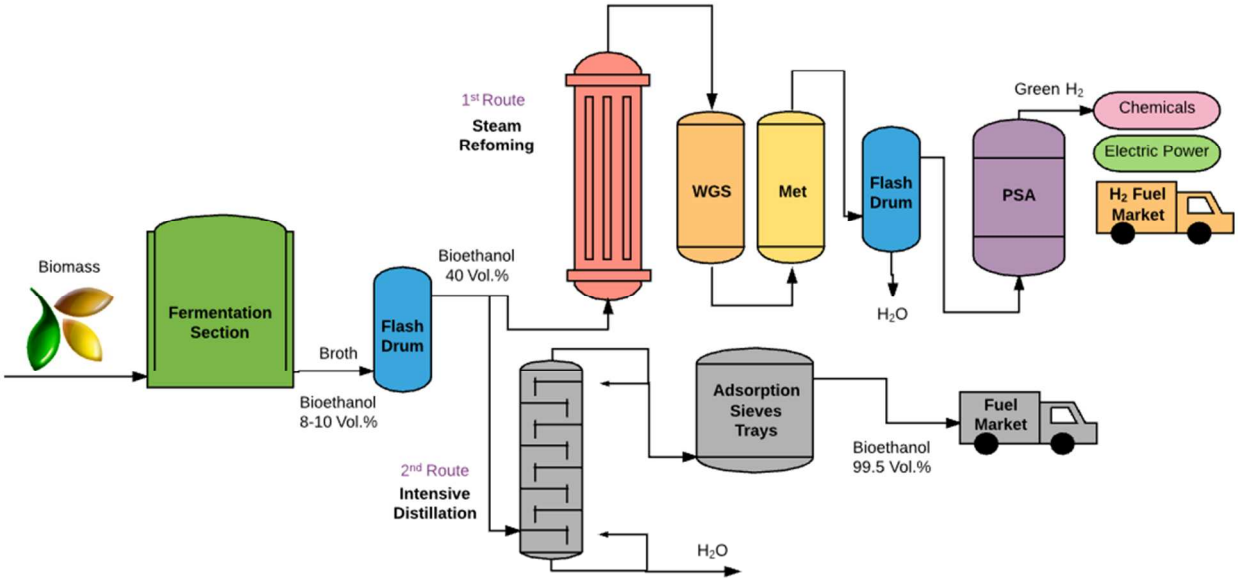

Fig. 2. Bioethanol-to-hydrogen process flowsheet.

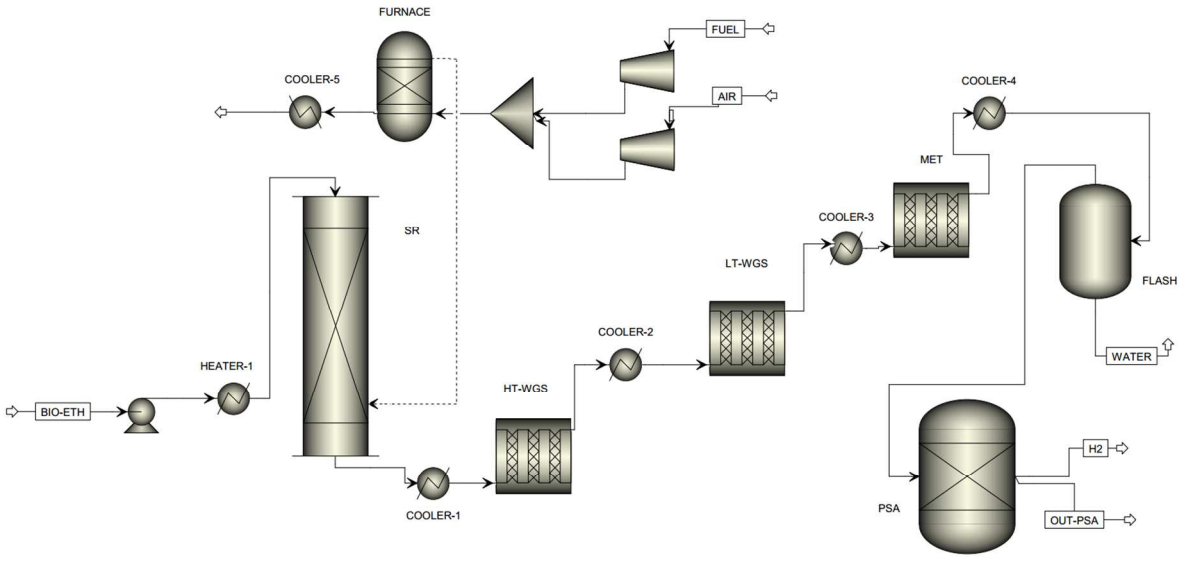

Fig. 3. Hydrogen production from bioethanol steam reforming flowsheet after heat integration (C and H after a given label identify the cold or hot side of the heat-exchanger).

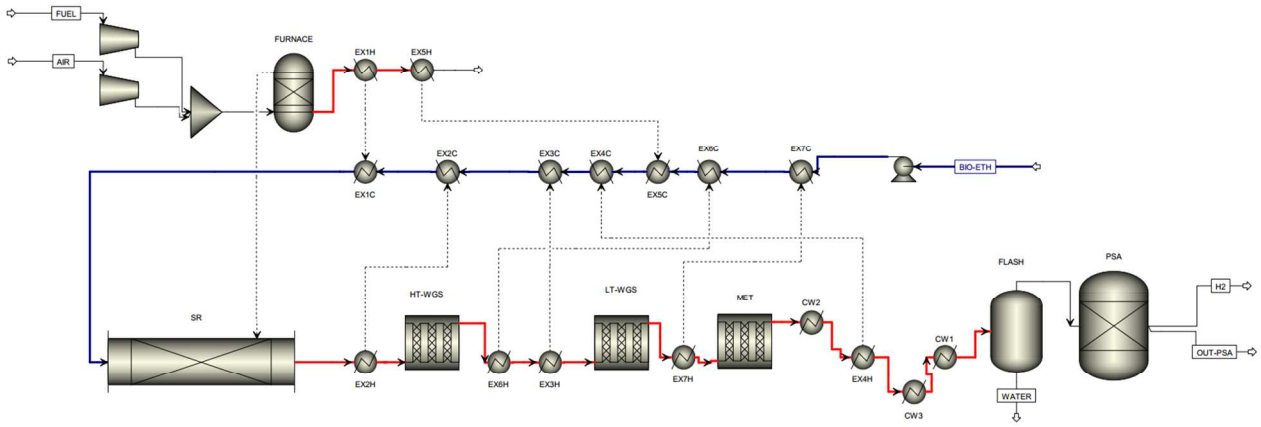

Fig. 4. Equipment purchase costs as base for capital expenditure calculation (top) and Operating (bottom) costs summary relative to raw materials and utilities, for the bioethanol steam reforming process without heat-integration using methane as fuel for the furnace. Utilities not shown are negligible.

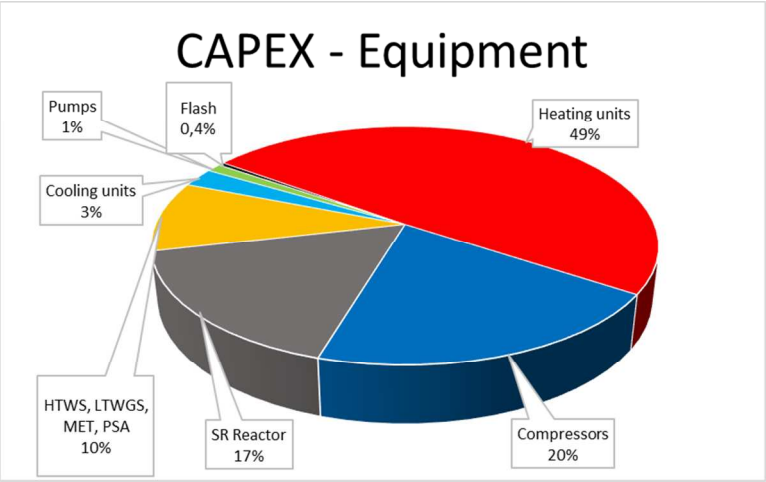

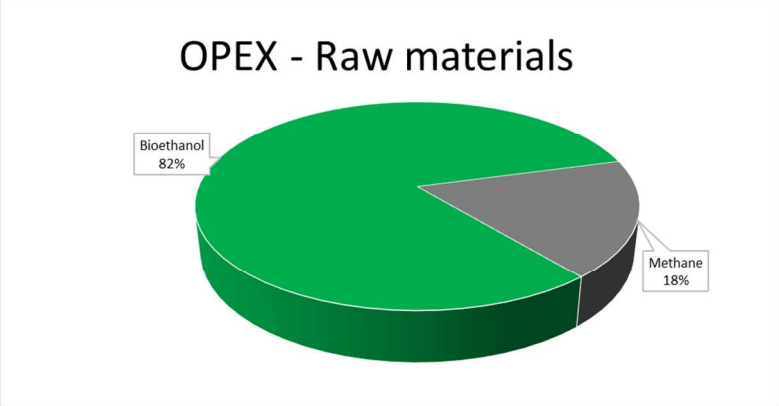

Fig. 5. Comparison of CAPEX and OPEX for the different scenarios. Values of CAPEX are reported as USD while OPEX and product sales as USD/year

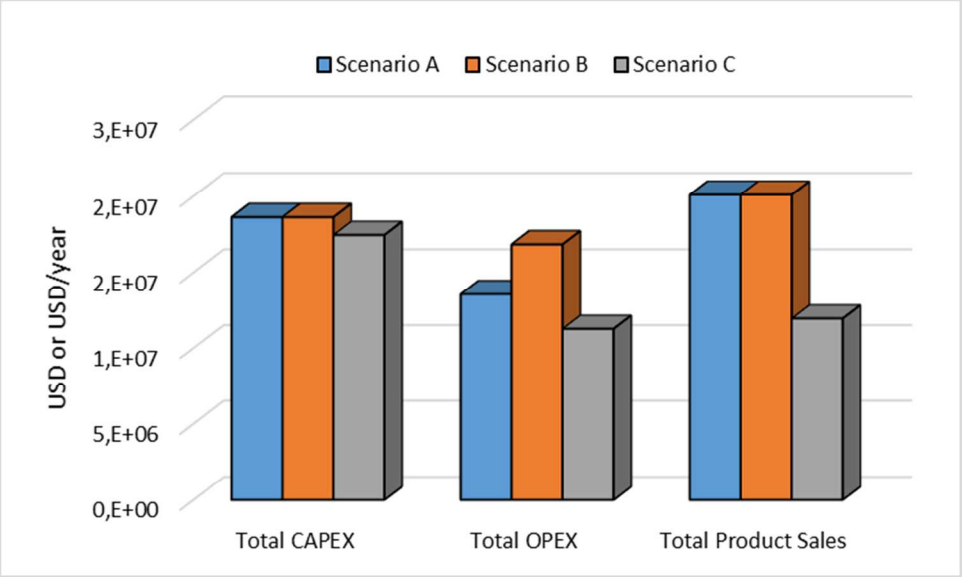

Fig.6. Capital cost summary for the bioethanol steam reforming process (scenario A) after heat-integration.

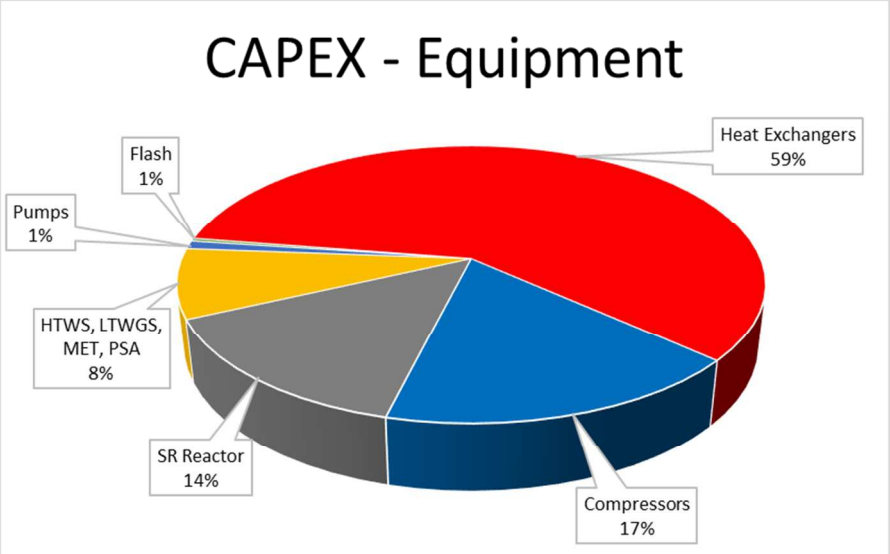

Fig. 7. Comparison of CAPEX and OPEX for the scenario A, before and after heat integration (HI) Values of CAPEX are reported as USD while OPEX and product sales as USD/year.

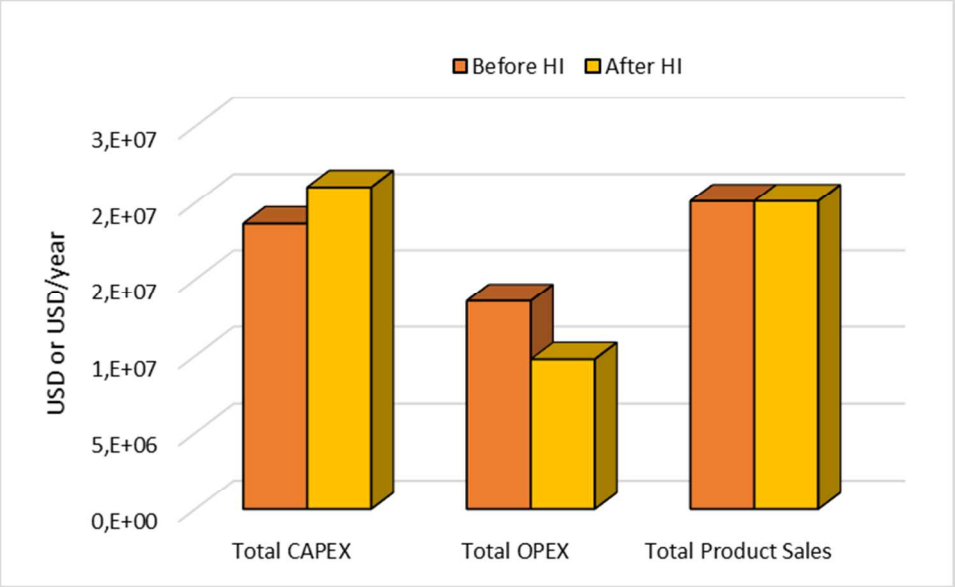

Fig. 8. Economic sensitivity analysis of the scenario A after heat integration. A) NPV and B) IRR after taxes dependence on cost variation of the various terms listed in the legend.